Constant-Temperature Free Energy Surfaces for Physical and Chemical Processes

Erik M. Boczko† and Charles L. Brooks, III*

Department of Chemistry, Carnegie Mellon University, Pittsburgh, Pennsylvania 15213

Received: December 2, 1992

A comparison between two methods for combining data from molecular simulations to generate free energy surfaces for physical and chemical processes is presented. The conventional "splicing" method is compared with a recently introduced histogram-based technique for the calculation of the free energy surface for folding a short peptide in vacuo. We present an extension of the weighted histogram analysis method, described recently by Kumar et al. (*J. Comput. Chem.* **1992**, *13*, 1101–1021), which is specialized to the case of constant-temperature simulations and generalized to multiple dimensions. Our data indicate that both methods produce identical results, at the qualitative level, for the folding free energy surface. However, the constant-temperature weighted histogram analysis equations we present here yield a smoother surface, incorporate all of the data from the simulations, and are generalized to multiple dimensions. We propose that these equations will provide a general framework for the calculation of free energy surfaces in multiple dimensions.

I. Introduction

One of the principal methods for generating free energy surfaces is to use importance sampling, better known as "umbrella" sampling, in conjunction with molecular dynamics or Monte Carlo simulations.[1,2] These techniques have been widely used to calculate reaction profiles for chemical processes in solution[3] as well as physical processes such as isomerization,[4] hydrophobic pairing,[5] and folding of small peptides.[6–9] For such calculations, a reaction coordinate is chosen and a series of independent simulations (or windows) are performed which span the relevant range of the reaction coordinate. To keep each of the individual simulations localized, a biasing potential in the reaction coordinate is imposed which restrains the system to remain near a prechosen value of the reaction coordinate. This potential generally changes from window to window, although the form of the potential often remains the same (e.g., harmonic). This results in a series of frequency distributions, or histograms, in the reaction coordinate, one from each window. These distributions are biased in the sense that they contain the effect of their respective restraining potentials. The goal is to unbias each of the windows for the effects of the restraining potential and to combine the data such that a single distribution over the entire range of the reaction coordinate is produced. This, in turn, is used to produce a free energy profile, for the process of interest.

The principal equation governing this procedure was described by Valleau and Torrie a number of years ago.[1] It is

$$P(r) = P^*(r)\exp[\beta V_{\mathrm{umb}}(r)]/\langle\exp[\beta V_{\mathrm{umb}}]\rangle_T \qquad (1)$$

$P(r)$ is the unbiased probability distribution, $P^*(r)$ is the biased probability, $V_{\mathrm{umb}}(r)$ is the restraining (umbrella) potential, and the angle brackets represent a constant-temperature (at T, with $\beta = 1/k_BT$) ensemble average over the biased system. If the average quantity in the denominator, which represents the reversible work required to impose the constraint, could be calculated, then the distributions could be combined analytically in any number of dimensions. However, this is not the case and alternate methods must be employed to combine simulation data from different windows to produce the desired probability distribution (and its attendant free energy surface).

In the conventional "splicing" method, adjacent distributions are matched using the constraint that overlapping portions of adjacent free energy surfaces must have matching slopes. The free energy surface for the ith window, $W_i(r)$, is related to the biased distribution function through the relationship

$$W_i(r) = -k_BT\ln[P^*_i(r)] - V_{\mathrm{umb}}(r) + C_i \qquad (2)$$

where k_B is the Boltzmann constant and C_i is the undetermined factor $k_BT\ln[\langle\exp[\beta V_{\mathrm{umb}}]\rangle_T]$ for the ith window. A common point is identified between two overlapping windows (from the region where the surfaces have matching slopes), and the data from the left distribution to the right of the chosen point is discarded and vice versa for the right distribution. The coefficients, C_i, are chosen to make the adjacent pieces of $W(r)$ equal at the common point.[2,6,8,10] The resultant spliced surface is an estimate for the free energy change along the predetermined reaction coordinate.

In more than one dimension the conventional splicing method just described is inadequate to combine data to yield a multidimensional free energy surface. A concise discussion of the problems encountered in using the splicing method in more than one dimension is given by Mezei et al.[10] We briefly outline the key components of the problems below. In one dimension, as described above, splicing free energy surfaces amounts to aligning two adjacent curves at a single point of overlap and shifting one relative to the other. In N dimensions, the surfaces will intersect along an $(N-1)$-dimensional seam (e.g., in two dimensions the surfaces will intersect along a line). If the surfaces are perfectly matched in slope, then this does not present a problem since a unique shifting constant can be found which aligns the identical seams of intersection. However, if the surfaces are not perfectly matched, e.g., due to small sampling errors, then a single constant will never match the seams along their entire length. Mezei et al.[10] suggested that a (unspecified) sample weighted least-squares fitting along the seam would yield an optimal solution to satisfying the continuity constraint. This approach is similar in spirit to the weighted histogram methods we discuss below.[11] However, this was never tried in practice.

An alternative to direct splicing in two dimensions has been investigated by Anderson and Hermans[9] for the case of the alanine dipeptide in water. In this formulation, several umbrella sampling calculations were performed, generating two-dimensional distributions in the dihedral angle space (∂, ψ). These distributions were then spliced together by performing conformational perturbation calculations between two specific configurations, one

* Author to whom correspondence should be addressed. Present address (while on sabbatical leave): The Scripps Research Institute, 10666 N. Torrey Pines Road, La Jolla, CA 92037.

† Department of Biological Sciences, Carnegie Mellon University, Pittsburgh, Pennsylvania 15213.

0022-3654/93/2097-4509$04.00/0

endpoint chosen from each of the distributions. This approach yields a single connection between two distinct conformational regions; however, it does not address questions regarding the overlap of adjacent distributions. Thus, one might anticipate problems similar to those just described when the conformational regions are not distinct. Furthermore, to provide single point connections between, say, N umbrella sampling calculations requires, in principle, $N(N-1)/2$ connecting free energy calculations. This is clearly a large amount of additional computation, which will also be prone to statistical sampling errors. For these reasons this method has not been used extensively to tackle multidimensional problems.

Recently, Kumar et al.[11] described a technique called the weighted histogram analysis method (WHAM) which represents a reformulating of an earlier optimal histogram approach developed by Ferrenberg and Swendsen[12,13] and is related to ideas posed by Bennet to extract thermodynamic information for molecular simulations through the use of histograms.[14] As the name implies, this technique combines simulation data from overlapping windows (such as windows of a conformational umbrella sampling simulation) by computing optimal weighting factors for each of the distributions (or histograms) over their common points. The weighting is carried out in a fashion which minimizes the squared error in the free energy estimate and has at least two advantages over the conventional splicing methods described above: first, none of the data from the simulation is discarded, and second, and perhaps most important, the method is not inherently limited to one dimension.

In the remainder of this paper we discuss the results of a comparison between the splicing and weighted histogram analysis methods as applied to the data from a 13-window umbrella sampling calculation of a blocked alanine tripeptide in vacuo using a distance-dependent dielectric to crudely mimic aspects of solvation. In the following section, we describe our specialization of the weighted histogram equations to the case of constant-temperature simulations and the generalization to multiple dimensions. In this case, histograms need only to be computed as a function of the reaction coordinate(s) and need not be binned in the energy variable, which is often problematic and has limited the success of this approach in applications to the thermodynamic properties of spin systems on large lattices.[15] In section III we describe a comparative test of the constant-temperature weighted histogram method and the conventional approach of splicing. The paper concludes with a discussion of the prospects for using this technique for multidimensional free energy calculations.

II. Constant-Temperature Weighted Histogram Analysis Equations

The equations governing the weighted histogram analysis method follow from consideration of an optimal (in a least-squares sense) means of combining data from several separate simulations.[11-14] A detailed derivation of these equations may be found in a recent publication by Kumar et al.[11,13] Our aim here is to describe a specialization of this methodology to the case where the temperature remains constant across all of the windows of the calculation. The original weighted histogram analysis method equations are

$$\Omega(E, r_1, r_2, ..., r_s) = \frac{\sum_{k=1}^{R} N_k(E, r_1, r_2, ..., r_s)}{\sum_{m=1}^{R} n_m \exp(F_m - \beta_m \sum_{j=0}^{L} \lambda_m^j V_j)} \quad (3)$$

and

$$P_{\{\lambda_m\}}(E, r_1, r_2, ..., r_s) = \Omega(E, r_1, r_2, ..., r_s) \exp(-\beta_m \sum_{j=0}^{L} \lambda_m^j V_j) \quad (4)$$

In eqs 3 and 4 above, we have followed a notation analogous to that of Kumar et al.[11] Ω is the density of states and is a function of the energy, E, for the unbiased reference system (which is equivalent to that under the influence of potential V_0) and the reaction coordinate in s dimensions, $(r_1, r_2, ..., r_s)$ [we assume that all of the biasing potentials are functions of the reaction coordinate $(r_1, r_2, ..., r_s)$]; N_k is the histogram of the energy and reaction coordinate in the kth window; n_m is the number of data samples used in computing the mth window histogram; the multiplicative coefficient λ_m^i is the coupling constant for the ith potential in window m. It is important to note that $\lambda_m^0 = 1$ for any m since the reference Hamiltonian is turned on in all of the windows. The function $P_{\{\lambda_m\}}(E, r_1, r_2, ..., r_s)$ is the unnormalized probability density for the mth window, and F_m is the scaled (by $-\beta_m$) free energy of the mth window (i.e., the shifting constant connecting adjacent windows at m). The notation $\{\lambda_m\}$ represents the set of coupling constants $i = 0, L$ used in window m. If we insert eq 3 into eq 4 and observe that all of the β_m are the same, constant temperature, then we can factor out $\exp(-\beta V_0)$ from the numerator and denominator, which cancel each other out. Now we observe that the only terms on the right-hand side that are a function of E are the histograms; the denominator no longer has any functions of E. We can now compute the marginal probability of the reaction coordinate by integrating over the energy degree of freedom E:

$$P_{\{\lambda_m\}}(r_1, r_2, ..., r_s) = \int_{P_{\{\lambda_m\}}} (E, r_1, r_2, ..., r_s)\, dE \quad (5)$$

This yields the first of our new weighted histogram equations

$$P_{\{\lambda_m\}}(r_1, r_2, ..., r_s) = \frac{\sum_{k=1}^{R} \int N_k(E, r_1, r_2, ..., r_s)\, dE \exp(-\beta \sum_{j=1}^{L} \lambda_m^j V_j)}{\sum_{l=1}^{R} nl \exp[F_l - \beta \sum_{j=1}^{L} \lambda_l^j V_j]} \quad (6)$$

and the second follows from the normalization condition for the probability distribution

$$\exp(F_m) = \int P_{\{\lambda_m\}}(r_1, r_2, ..., r_s)\, dr_1 dr_2 ... dr_s \quad (7)$$

The integral over energy for the kth histogram simply yields the histogram as a function of the reaction coordinate. Thus, the constant-temperature weighted histogram equations are independent of the reference system energy, and one need only compute histograms as a function of the reaction coordinate. Given the set of R s-dimensional histograms, from simulations $m = 1,R$, the optimal solution for the undetermined coefficients (F_m) comes from the self-consistent solution of eqs 6 and 7. We note that eqs 6 and 7 can also be arrived at by simply omitting the dependence on V_0, as was shown in refs 12 and 13.

III. Comparison of Conventional Splicing and Weighted Histogram Analysis Methods: Helix Formation in a Blocked Alanine Tripeptide

An umbrella sampling calculation was performed for the blocked tripeptide AMN-(ALA)$_3$-CBX. This peptide and its thermodynamic behavior have been extensively studied within our group.[7,8] AMN is an amino methyl blocking group, and CBX is a carboxy methyl blocking group. These groups allow the tripeptide to form an O1 to H5 hydrogen bond and mimic

TABLE I: Harmonic Restraint Parameters and Initial Conformations for the Blocked Alanine Tripeptide in Umbrella Sampling Simulations[a]

window	R_{center}	$R_{initial}$	ϕ_1	ψ_1	ϕ_2	ψ_2	ϕ_3	ψ_3
1	1.8	2.0	-85	-37	-70	-48	-81	-53
2	2.8	2.75	-100	-38	-73	-30	-109	11
3	3.8	3.5	-65	-14	-108	-59	-84	-71
4	4.8	5.0	-82	-73	-95	-39	-86	71
5	5.8	5.75	-87	-29	-103	-7	-151	106
6	6.8	6.5	-98	-82	-48	-55	-97	156
7	7.8	8.0	-79	-85	-105	13	-76	155
8	8.8	8.75	-138	-47	-108	-29	-97	144
9	9.8	9.5	-79	-70	-174	-45	-109	-180
10	10.8	11.0	-127	-76	-151	-56	-72	-179
11	11.8	11.75	-136	167	-86	-76	-160	-178
12	12.8	12.5	-153	179	-137	140	-117	-136
13	13.8	13.25	-152	167	-124	174	-101	-139

[a] Initial conditions are shown for each of the 13 windows. Column 2 indicates the harmonic restraint reference position; the restraint force constant was 1.20 kcal mol^{-1} Å^{-2} for all windows. Column 3 indicates the initial r(O1–H5) distance of the tripeptide in each window. Initial values of the six ϕ–ψ angles are shown in the remaining columns.

one turn of an alpha helix. The O1 to H5 hydrogen-bonding distance, denoted r(O1–H5) or simply r, was chosen as a reaction coordinate for the folding of this peptide. The umbrella sampling calculations consisted of 13 independent windows. A canonical set of initial configurations which spanned the reaction coordinate, listed in Table I, were generated and an appropriate one was used in each window of the calculation. A harmonic restraining potential was imposed in each of the 13 windows; the force constants were the same across all of the windows, k = 1.20 kcal mol^{-1} Å^{-2}. The reference positions are detailed in Table I. Each window was equilibrated for 10 000 steps with a 2-fs time step and then simulated for an additional 2 million steps with the same step size. Data were collected every 10 steps for a total of 200 000 data points per window. The standard CHARMM potential (PARAM19) was used with a distance-dependent dielectric, $\epsilon = r$.[16] The nonbonded interactions were truncated at 8.0 Å with van der Waals switching and electrostatic shifting functions.[16] The Verlet algorithm[17] was used to integrate the equations of motion, and the SHAKE[18] algorithm was employed to constrain hydrogen bond lengths. All calculations were performed on an IBM RS6000 workstation with the CHARMM22 molecular mechanics program.

The splicing algorithm used was written by the authors and works in the most naive way possible. The algorithm finds the point of maximum overlap between adjacent biased probability distributions and discards the overlapping data. Then it unbiases the remaining data in each window with the appropriate Boltzmann factors, takes the negative natural logarithm, and computes the shifting constants from left to right (in the reaction coordinate) of the adjacent segments.

The constant-temperature weighted histogram analysis equations (eqs 6 and 7) are a set of coupled nonlinear equations and must be iterated to convergence. Convergence is judged by specifying a tolerance for the absolute difference between values of the shifting coefficients, F_m, between iterate α and $\alpha + 1$. For this study the tolerance value for convergence was set to zero, within machine single precision, and convergence was observed with at most 800 iterations, about 20 min wall clock time. In related studies we noted that this level of tolerance was not necessary to achieve converged results; values of 0.005 for the tolerance were sufficient to converge the result within 20 iterations and less than 1 minute wall clock time.[19] Different choices for the initial F_ms did not influence the convergence behavior, as noted by Kumar et al. in their formulation of the problem.[11] The bin size for the histograms was kept constant at 0.05 Å for the data shown. The algorithm for the iterative optimization was coded in FORTRAN 77. A copy of this program is available from the authors upon request.

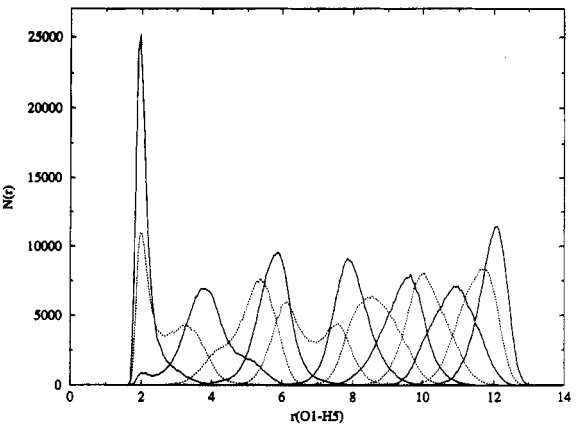

Figure 1. Thirteen-piece-wise biased probability densities in the reaction coordinate r(O1–H5). Densities from even-numbered windows are shown as dotted lines, and those from odd-numbered windows are shown as solid lines for clarity. The reference centers for each biased sampling are given in Table I.

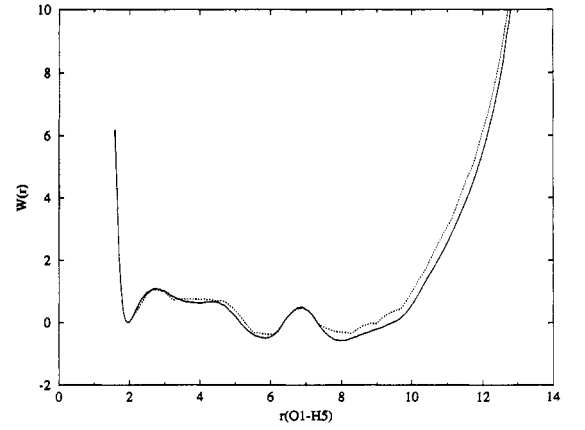

Figure 2. Comparison of free energy surfaces from the constant-temperature weighted histogram analysis method and conventional splicing. The histogram blended surface is shown as a solid line and the spliced surface as the dotted line. The curves have arbitrarily been set equal at r(O1–H5) = 2 Å. Both curves were computed using all of the 200 000 data points per window (2 million time steps) and included all 13 of the windows.

The 13 biased probability distributions are shown in Figure 1. The distributions are well interpenetrated. While this overlap is essential for proper splicing, it is at the same time wasteful since much of the data is discarded. Figure 2 shows the associated free energy surfaces computed with the new constant-temperature weighted histogram analysis equations and with conventional splicing. The curves have been set equal to one another at r = 2 Å arbitrarily for comparison. Previously, it has been shown that for small values of the coordinate r the peptide is unambiguously in an α-helical conformation, and for large values of r, >8 Å, the peptide is in an extended β conformation.[7,8]

It is immediately evident that the constant-temperature weighted histogram analysis method produces a much smoother surface. The spliced surface contains several edges where adjacent distributions were joined together, and this edginess is often a concern since systematic errors at the splice junctions could potentially cause large errors in a calculated equilibrium constant, for example. Reassuringly, the two methods produce qualitatively identical and quantitatively similar results. The surfaces differ by at most 0.1 kcal mol^{-1} from the α-helical manifold at r = 2 Å to the transition state, consisting of multiple C_{7eq} and/or C_{7ax} conformations in the three sets of (ϕ, ψ), and into extended the β conformation at r = 7 Å. The surfaces differ most dramatically, by at most 0.25 kcal mol^{-1}, along the extended-state manifold, which is probably due to the "directional" nature of our splicing algorithm and accumulated splicing errors. Both surfaces

TABLE II: Mole Fraction for Helix, C_7/turn, and Extended States Computed from Spliced and Constant-Temperature Weighted Histogram Analysis Surfaces[a]

method	segment[b]	χ_{eq}^{helix}	$\chi_{eq}^{C_7/turn}$	$\chi_{eq}^{extended}$
splice	0–500000	0.049 (39%)	0.549 (23%)	0.402 (15%)
	0–1000000	0.141 (77%)	0.680 (53%)	0.179 (62%)
	0–1500000	0.112 (40%)	0.574 (29%)	0.314 (34%)
	0–2000000	0.080 (0%)	0.445 (0%)	0.475 (0%)
histogram	0–500000	0.033 (44%)	0.494 (25%)	0.474 (13%)
	0–1000000	0.097 (65%)	0.650 (65%)	0.253 (54%)
	0–1500000	0.078 (33%)	0.498 (26%)	0.424 (23%)
	0–2000000	0.059 (0%)	0.394 (0%)	0.547 (0%)

[a] Mole fractions computed from eq 8; helical region defined to be r(O1–H5) < 3 Å, C_7/turn region 3 Å < r(O1–H5) < 7 Å; extended region r(O1–H5) > 7 Å. The number given in parentheses following the equilibrium constant is the absolute relative error from the longest simulation segment. [b] The segment numbers refer to the number of time steps used in computing the free energy surface.

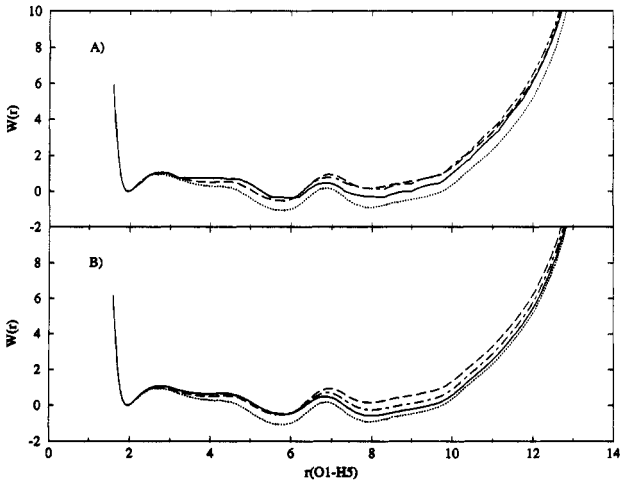

Figure 3. Convergence of the cumulative surfaces computed using (A) conventional splicing and (B) the constant-temperature weighted histogram analysis method blending. The dotted line is for the first 50 000 data points per window, the dashed line is for the first 100 000 data points per window, the dot-dashed line is for the first 150 000 data points, and the solid line is for all of the data.

reproduce the three minima and the two transition states, although we expect that a helix to coil equilibrium constant calculated from the two surfaces would differ quantitatively, with the equilibrium constant from the constant-temperature weighted histogram analysis method surface predicting a larger extended-state population. In fact, the free energy difference between the α-helical and extended β conformation, calculated from the ratio of mole fractions given by eq 8 and the data from Table II, is -1.06 kcal mol^{-1} from splicing and -1.32 kcal mol^{-1} from the constant-temperature weighted histogram surface (when all of the data are used). Thus, quantitative predictions based on these surfaces differ by at most 0.27 kcal mol^{-1}. We take this similarity to be a cross-validation of both methods.

It is worth pointing out that in practice many fewer than 2 million steps of dynamics are carried out over an entire umbrella sampling calculation, and consequently much less sampling per window is used. Therefore, it is instructive to look at successive segments of the data and examine how the surfaces, from both methods, converge to the final result shown in Figure 2. In Figure 3A we show the convergence behavior for four cumulative spliced surfaces. The first spliced surface, shown as the dotted line, consists of the first 500 000 steps from each window. The second surface, shown as the dashed line, consists of the first 1 million steps, and so on. Besides displaying a marked edginess, the trend in the cumulative spliced surfaces is first to exaggerate the minimum at r = 6 Å and then to overestimate the maximum at r = 7 Å and the extended-state minimum beyond. The convergence profile for the constant-temperature weighted histogram analysis is shown in Figure 3B, and the same trend is evident. We take this as strong evidence for the conclusion drawn from the results in Figure 2, namely, that both methods are yielding correct and very similar results. In addition, Figure 3 suggests that systematic errors introduced by splicing are minimal in our one-dimensional surfaces. Without the comparative analysis from the constant-temperature weighted histogram method, one might well attribute the overestimation of the minimum at r = 6 Å in the first spliced curve to a systematic error introduced at the splice junction around r = 3 Å. The constant-temperature weighted histogram analysis results show exactly the same trend and thus help to convince us that this feature of the surface is most likely a reflection of some transient nonequilibrium property of the peptide dynamics.

Another means of judging convergence of the surfaces is to probe their underlying mole fraction. We estimate this property by computing the integral of the Boltzmann factor of each surface between well-defined limits[7,8]

$$\chi_{eq}^{ij} = \frac{\int_{r_i}^{r_j} \exp[-\beta W(r)]\, dr}{\int_{\text{all } r} \exp[-\beta W(r)]\, dr} \tag{8}$$

where r_i and r_j denote the beginning and end of a particular conformational manifold (denoted either by ij or by a conformational designation such as helical) and $W(r)$ is the free energy surface resulting from either the splicing or constant-temperature weighted histogram analysis methods. In Table II we show the mole fractions associated with the α-helical manifold, the intermediate C_7/turn manifold, and the extended β manifold for this model calculation. Our results show that a maximum relative error (measured relative to the 2 million step simulation surfaces) of 77% is achieved for these constants. This occurs for the intermediate length sampling of 1 million time steps per window. Furthermore, we see that the differences between the mole fractions from the splicing surfaces and the constant-temperature weighted histogram analysis surfaces are small. These observations suggest that quantitative differences between mole fractions computed from free energy surfaces can be significant, even for extremely long simulations such as those presented here. Thus, the cumulative behavior of mole fractions may provide a sensitive test of the quantitative convergence of these surfaces. However, we note that despite the poor quantitative agreement, all computed mole fractions yield the same qualitative picture for the conformational preferences for this peptide, namely, the helical state is of lower population than either the turn or extended regions, which themselves are roughly equal.

IV. Conclusions

In this paper, we have presented an extension of the weighted histogram analysis method recently described by Kumar et al.[11] for the special case of constant temperature and generalized this formulation to multiple dimensions. Major advantages of the constant-temperature weighted histogram analysis formulation are that it eliminates the necessity of considering histograms in an energy variable for conformational free energy calculations and it is not limited to a single dimensional reaction coordinate. We have demonstrated that results from splicing and the constant-temperature weighted histogram analysis blending are qualitatively identical. We take this favorable comparison between surfaces generated by both methods as a cross-validation.

By performing very long umbrella sampling simulations on the blocked alanine tripeptide, we have examined the convergence behavior of both the free energy surface and quantities derived from it, i.e., mole fractions. Our findings suggest that converged free energy surfaces (in a qualitative sense) are achieved even for the shortest simulation sequences we consider here (500 000

samples). When the mole fractions are considered, we observe that quantitative convergence is still elusive; however, qualitative behavior is achieved with the shorter calculations.

The fact that the constant-temperature weighted histogram analysis equations are rather easily generalized to multiple dimensions, as the equations in section II demonstrate, leads us to suggest that this formulation will overcome one of the major hurdles facing such computations. The splicing of multidimensional probability distributions is not straightforward (see, for example, Mezei et al.),[10] and to the best of our knowledge a multidimensional free energy surface has never been produced by the Valleau and Torrie method. We are at present investigating the applicability of the formulation presented here to the case of a multidimensional free energy surface generated by placing the blocked alanine tripeptide at the interface of a water–hydrophobic wall. We will report on these findings in a future publication.

Acknowledgment. Helpful discussions with Shankar Kumar and Melvin Muroff are gratefully acknowledged. E.M.B. also acknowledges support from an NIH predoctoral training grant (GM-08067). Partial financial support from the NIH (GM-37554) and the Alfred P. Sloan Foundation is also acknowledged by C.L.B.

References and Notes

(1) Valleau, J. P.; Torrie, G. M. In *Statistical Mechanics, Part A*; Berne, B. J., Eds.; Plenum Press: NY, 1977, pp 169–194.
(2) Beveridge, D. L.; DiCapua, F. M. *Annu. Rev. Biophys. Biophys. Chem.* **1989**, *18*, 431–492.
(3) Jorgensen, W. L. *Acc. Chem. Res.* **1989**, *22*, 184–189.
(4) Jorgensen, W. L. *J. Phys. Chem.* **1983**, *87*, 5304–5314.
(5) Smith, D. E.; Zhang, L.; Haymet, A. D. J. *J. Am. Chem. Soc.* **1992**, *114*, 5875–5876.
(6) Tobias, D. J.; Brooks, C. L., III. *J. Mol. Biol.* **1991**, *216*, 783–796.
(7) Tobias, D. J.; Sneddon, S. F.; Brooks, C. L., III. In *Advances in Biomolecular Simulations*; American Institute of Physics: Obernai, France, 1991; Vol. 239.
(8) Tobias, D. J.; Brooks, C. L., III. *Biochemistry* **1991**, *30*, 6059–6070.
(9) Anderson, A. G.; Hermans, J. *Proteins* **1988**, *3*, 262–265.
(10) Mezei, M.; Mehrotra, P. K.; Beveridge, D. L. *J. Am. Chem. Soc.* **1985**, *107*, 2239–2245.
(11) Kumar, S.; Bouzida, J.; Swendsen, R.; Kollman, P.; Rosenberg, J. *J. Comput. Chem.* **1992**, *13*, 169–194.
(12) Ferrenberg, A. M.; Swendsen, R. H. *Phys. Rev. Lett.* **1989**, *63*, 1195–1198.
(13) Ferrenberg, A. M. Ph.D., Carnegie Mellon University, 1989.
(14) Bennet, C. M. *J. Comput. Phys.* **1976**, *22*, 245–268.
(15) Hu, C. *Phys. Rev. Lett.* **1992**, *69*, 2739–2742.
(16) Brooks, B. R.; Bruccoleri, R. D.; Olafson, B. D.; States, D. J.; Swaminathan, S.; Karplus, M. *J. Comput. Chem.* **1983**, *4*, 187–217.
(17) Verlet, L. *Phys. Rev.* **1967**, *159*, 98–103.
(18) Ryckaert, J.-P.; Ciccotti, G.; Berendsen, H. J. C. *J. Comput. Phys.* **1977**, *23*, 327–341.
(19) Brooks, C. L.; Nilsson, L. Unpublished results.